Photo-responsive Liquid Crystalline Epoxy Networks with Shape Memory Behavior and Dynamic Ester Bonds

Yuzhan Li[a], Orlando Rios[b], Jong K. Keum[c], Jihua Chen[c], and Michael R. Kessler[a,*]

[a] School of Mechanical and Materials Engineering, Washington State University, Pullman, WA 99164, USA

[b] Deposition Sciences Group, Oak Ridge National Laboratory, Oak Ridge, TN 37831, USA

[c] Center for Nanophase Materials Sciences, Oak Ridge National Laboratory, Oak Ridge, TN 37831, USA

[*] PO Box 642920, Pullman, WA, 99164-2920; Phone (509) 335-8654; Email: MichaelR.Kessler@wsu.edu

ABSTRACT

Functional polymers are intelligent materials that can respond to a variety of external stimuli. However, these materials have not yet found wide-spread real world applications because of the difficulties in fabrication and the limited number of functional building blocks that can be incorporated into a material. Here we demonstrate a simple route to incorporate three functional building blocks (azobenzene chromophores, liquid crystals, and dynamic covalent bonds) into an epoxy-based liquid crystalline network (LCN), in which an azobenzene-based epoxy monomer is polymerized with an aliphatic di-carboxylic acid to create exchangeable ester bonds that can be thermally activated. All three functional building blocks exhibited good compatibility and the resulting materials exhibits various photomechanical, shape memory, and self-healing properties because of the azobenzene molecules, liquid crystals, and dynamic ester bonds, respectively.

KEYWORDS: liquid crystalline networks, photo-responsive, shape memory, self-healing, thermomechanical properties

1. INTRODUCTION

Functional polymers include stimuli-responsive materials exhibiting a variety of properties, such as shape memory,[1-2] self-healing,[3-4] switchable wettability,[5-6] reversible adhesion,[7-8] and redox-controlled permeability,[9] among others. These remarkable properties make them excellent candidates for a broad range of applications, such as actuators, drug delivery systems, and self-assembling devices.[10-11] However, real world applications of these materials are still limited because of the number of functional building blocks that can be incorporated into a material and the difficulties in fabricating and coordinating these functional building blocks.

Liquid crystalline networks (LCN) are versatile functional materials because of the unique properties of the liquid crystalline (LC) molecules, e.g., self-organization, reversible phase transition, and macroscopic orientation under external fields.[12-13] The coupling between

LC molecules and polymer networks allows these remarkable properties to be transferred to the bulk material, which results in a number of functional LCNs that are thermally-responsive and are able to change their shape reversibly upon temperature cycling.[14]

In recent years, using light to induce shape change has received a lot of attention because light can be controlled both remotely and instantly.[15-17] The incorporation of photo-responsive chromophores, such as azobenzene, into LCNs allows the material to convert light energy into mechanical work because of the transformation between two geometrically different azobenzene isomers upon light irradiation. The degree of this transformation can be controlled by selecting an appropriate irradiation wavelength (between the ultraviolet and the blue region), which in turn will induce bending[18] or re-orientation[19] of the azobenzene molecules and subsequently result in a macroscopic shape change of the bulk LCN materials, including bending,[20-22] twisting,[23] and oscillating.[24] However, almost all photo-responsive LCNs are polysiloxane and polyacrylate-based systems. In some cases, the high crosslink density of the network does not allow the liquid crystals to go through a reversible phase transition, thereby affecting the potential functionality of these materials. In addition, these siloxane and acrylate-based LCNs cannot be reprocessed because of their covalently crosslinked structure, which makes it impossible to reshape or repair the material.

There has been growing interest in using dynamic covalent chemistries to design polymers because it allows for the covalent bonds to be broken and reformed upon application of external stimuli.[25-26] Dynamic ester bonds have recently been incorporated into epoxy and LC epoxy networks. They have shown to be effective in improving reprocessability of the material.[27-28]

In this work, we designed a simple method and prepared a multifunctional LCN using three different functional building blocks (azobenzene chromophores, liquid crystals, and dynamic ester bonds), which allowed to program material responses to external stimuli at the molecular level. Without additional tuning and processing, the material exhibited various photomechanical behaviors, dual-stimuli induced shape memory and self-healing properties, and excellent reprocessability.

2. EXPERIMENTAL SECTION

2.1 Preparation of LCN Films.

The LCNs were synthesized by curing of an azobenzene-based epoxy monomer (4,4'-diglycidyloxyazobenzene, AE) and a di-carboxylic acid curing agent (sebacic acid, SA) at an epoxy/carboxylic acid ratio of 1:1. A ring-opening/transesterification catalyst (1,5,7-triazabicyclo[4.4.0]dec-5-ene, TBD) was used at an amount of 5 mol% of carboxylic acid groups. The three chemicals were dissolved in acetone and sonicated for 30 min followed by evaporation of the acetone at room temperature. The powder mixture was further grinded using a pestle and mortar. LCN films were prepared using the parallel plate fixture of a strain-controlled rheometer (ARES G2, TA Instruments). The thickness of the film was controlled by the gap of the parallel plates. The material was cured at 170 °C for 1h in ARES G2, then moved to a convection oven and cured at 200°C for 3h.

2.2 Structure Characterization.

Two-dimensional X-ray scattering measurements were carried out using an Anton Paar SAXSess mc^2. The scattering beam was recorded on an imaging plate (Multi-sensitive Storage

Phosphor) and read using an imaging plate reader. The X-rays were generated at 40 kV/50 mA and the wavelength of the used X-ray beam was λ=1.541 Å (Cu-Kα radiation). The structure of LCNs at strain values of 0%, 100 %, 200 %, and 400 % was examined using both small angle X-ray scattering (SAXS) and wide angle X-ray scattering (WAXS) configurations. TEM samples were prepared by embedding LCN in a low viscosity resin before microtomed into 75-nm-thick slices and placed onto holey carbon supported copper grids. The samples were examined using a Zeiss Libra 120 TEM at 120 kV under low beam conditions. Dark field images were taken 0.5/nm objective aperture centered over the strongly diffracted beam at approximately 2.2/nm. Typical exposure times are 0.5 s for electron diffraction, 1 s for bright field imaging, and up to 8 s for carbon mapping in energy filtered imaging.

2.3 Photomechanical Behavior Characterization.

UV-Vis spectra of the AE monomer (dissolved in chloroform) were measured using a UV-Vis spectrometer (Lambda 25, PerkinElmer). The light source used for the photomechanical characterization was generated by a UV curing lamp system with a 320-500 nm internal filter (OmniCure S2000, Excelitas Technologies). The light was guided into an adjustable collimating adapter (Lumen Dynamics) and then passed through a bandpass filter (355 nm or 442 nm) and a polarized beamsplitter cube (Thorlabs). The final intensity of the light was measured using either a blue light radiometer (Solartech) or a UV radiometer (UV Process Supply).

2.4 Thermomechanical Property Characterization.

The thermal properties of AE monomer and the LCNs were determined using a differential scanning calorimeter (Discovery DSC, TA Instruments) under a nitrogen purge of 20 mL/min. A heat-cool-heat cycle with a ramp rate of 20 °C/min was used. T_g and T_{lc} were determined from the second heating scan. Static tensile tests were carried out using the ARES G2 rheometer in a film tension geometry. The LCN film was heated to 80 °C (between T_g and T_{lc}) and the axial force was measured under a strain ramp rate of 0.002 s^{-1}. Cyclic thermomechanical tensile tests were carried out using ARES G2 in a film tension geometry. The LCN film was heated to 140 °C (above T_{lc}), and then a constant force of 0.01 N was applied. Then the temperature was decreased to 80 °C at a cooling rate of 1 °C/min and then increased to 140 °C again at a heating rate of 1 °C/min. The strain of the LCN film was measured during the temperature cycling. Cyclic thermomechanical compression tests were carried out using a thermomechanical analyzer (Q400EM, TA Instruments).

3. RESULTS AND DISCUSSION

3.1 LCN Synthesis

The synthesis route for the combination of the three selected functional building blocks is depicted in Figure 1a. The azobenzene-based epoxy monomer (AE) was synthesized (Supplementary Figure S1 and S2) and polymerized with an aliphatic di-carboxylic acid (SA) to form an LCN. A ring-opening/transesterification catalyst (TBD) was incorporated into the system to promote the formation of an LC phase as well as to activate the dynamic ester bonds created by the epoxy-acid reaction. As shown in Figure 1a, the reaction between AE and SA involved two major competing reactions, including the ring-opening reaction of the epoxy by carboxylic acid and the crosslinking reaction through the hydroxyl groups created by the opened

epoxy rings. Provided that AE itself is not liquid crystalline (Supplementary Figure S3), the ring-opening reaction of AE by SA is crucial for an LC phase formation because the addition of SA increases the mobility of the AE molecules by introducing flexible aliphatic chains and facilitates their self-organization into an ordered LC phase. The use of TBD was equally important to facilitate LC phase formation as it accelerated the ring-opening reaction and prevented extensive crosslinking in the early stage of the curing reaction (Supplementary Figure S4). LCN samples were synthesized by one-pot curing of the three components, which provided a simple way to prepare LCNs. Fully cured LCNs exhibited a glass transition temperature (T_g) of 51 °C and an LC phase transition temperature (T_{lc}) of 103 °C (Supplementary Figure S5). A smectic LC polydomain structure was confirmed by both polarized optical microscopy (POM, Supplementary Figure S6) and two-dimensional small-angle/wide-angle X-ray scattering (2D SAXS/WAXS, Figure 3d and Supplementary Figure S7).

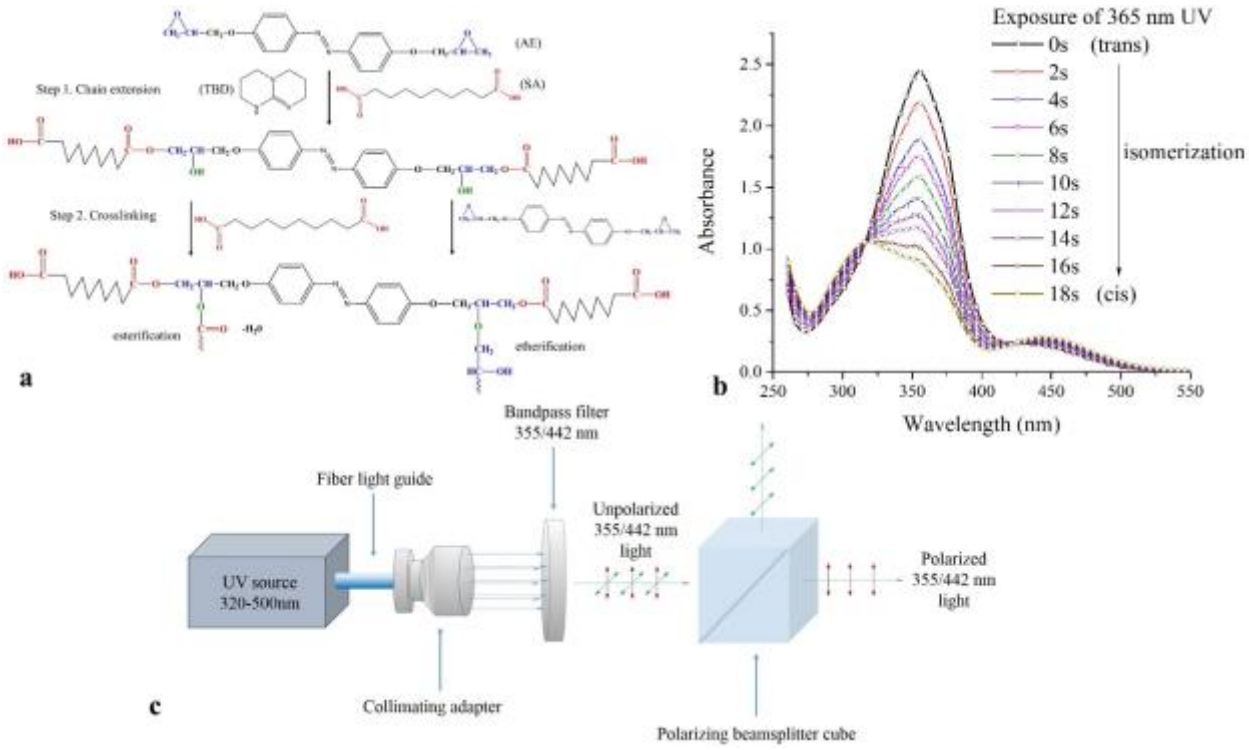

Figure 1. Structure and characterization of epoxy-based azobenzene monomer and LCNs. a) Synthesis route and reaction mechanism of multifunctional LCNs. b) UV-Vis absorption spectra of AE monomer at different UV (365 nm) exposure times. c) Optical setup for photomechanical characterization.

3.2 Photo-responsive Behavior

As mentioned earlier, the photomechanical behavior of azobenzene functionalized polymers is determined by the conformational change between a planar, rod-like, trans-isomer with a molecular length of 9 Å and a non-planar, bent, cis-isomer with a molecular length of 5.5 Å. This transformation can be controlled by the wavelength of the incident light. Exposure to UV light usually leads to a trans-cis isomerization, resulting in bending of the azobenzene molecules.

The use of blue light, on the other hand, usually leads to a trans-cis-trans isomerization, where trans-azobenzene molecules are initially transformed to cis-isomers but return back to the trans-state with a preferred orientation. In addition, the use of linear polarized light allows for selective azobenzene molecules to be exposed to light, enabling precise control of the photomechanical behavior.

In order to better understand the photo-isomerization process, absorption spectra of the synthesized AE monomer were characterized using ultraviolet-visible (UV-Vis) spectroscopy, as shown in Figure 1b. Prior to UV irradiation, trans-AE was the predominant isomer as indicated by the strong peak at 355 nm caused by the $\pi \rightarrow \pi^*$ absorption band of the trans-isomer. As the UV exposure time increased, the intensity of this peak decreased significantly, indicating a reduction of trans-isomers. Meanwhile, a new peak was observed at 444 nm corresponding to the $n \rightarrow \pi^*$ absorption band of the cis-isomer. The increase in peak intensity indicated a gradual buildup of cis-AE isomers with UV irradiation. The comparison of absorption spectra of trans- (black line) and cis- (brown line) isomers shows that in the blue light region (440 to 495 nm), both isomers exhibited nearly equivalent light absorption, which has been known to promote the trans-cis-trans isomerization of the azobenzene molecules.[19]

To investigate the photomechanical behavior of the LCNs, a optical system was constructed as shown in Figure 1c. It can produce either polarized blue light at 442 nm or polarized UV light at 355 nm. Figure 2a shows the blue light induced deformation of the LCNs. Depending on the polarization direction of the incident light, the LCN film bent either toward or away from the light source (Supplementary Video S1 and S2). The mechanism of this bidirectional bending behavior is illustrated in Figure 2b. It has been known that azobenzene molecules can be aligned perpendicularly to a polarized blue light.[29] However, because of the high extinction coefficient of azobenzene molecules, most of the incident photons were absorbed at the top layer of the LCN film, resulting in a re-orientation of the azobenzene molecules only on the light-fronting surface.[30] When the direction of polarization (E) was parallel to the long axis (x) of the LCN film, the azobenzene molecules on the light-fronting surface were oriented perpendicular to the polarization direction, leading to a contraction of the LCN film on the surface layer. The rest of the LCN film, however, remained unchanged; this difference caused the bending of the LCN film toward the light source. In contrast, when E and x were perpendicular, the re-orientation resulted in an expansion of the LCN film on the light-fronting surface and the net effect was the bending of the LCN film away from the light source. Because of the reversible nature of the trans-cis-trans isomerization process, the direction of a bent LCN film can be altered by changing the direction of the light polarization (Supplementary Video S3 and S4).

Figure 2c shows the UV light induced deformation of the LCNs and the associated mechanism is shown in Figure 2d. The bending direction can be precisely controlled by the polarization direction of the UV light. As shown in Figure 2d, the use of polarized light resulted in a selective absorption, where only azobenzene molecules parallel to the polarization direction of the UV light were able to absorb light energy and transform to cis-isomers. The bending of these molecules resulted in a contraction of the top surface and caused bending of the LCN film in the direction of polarization.

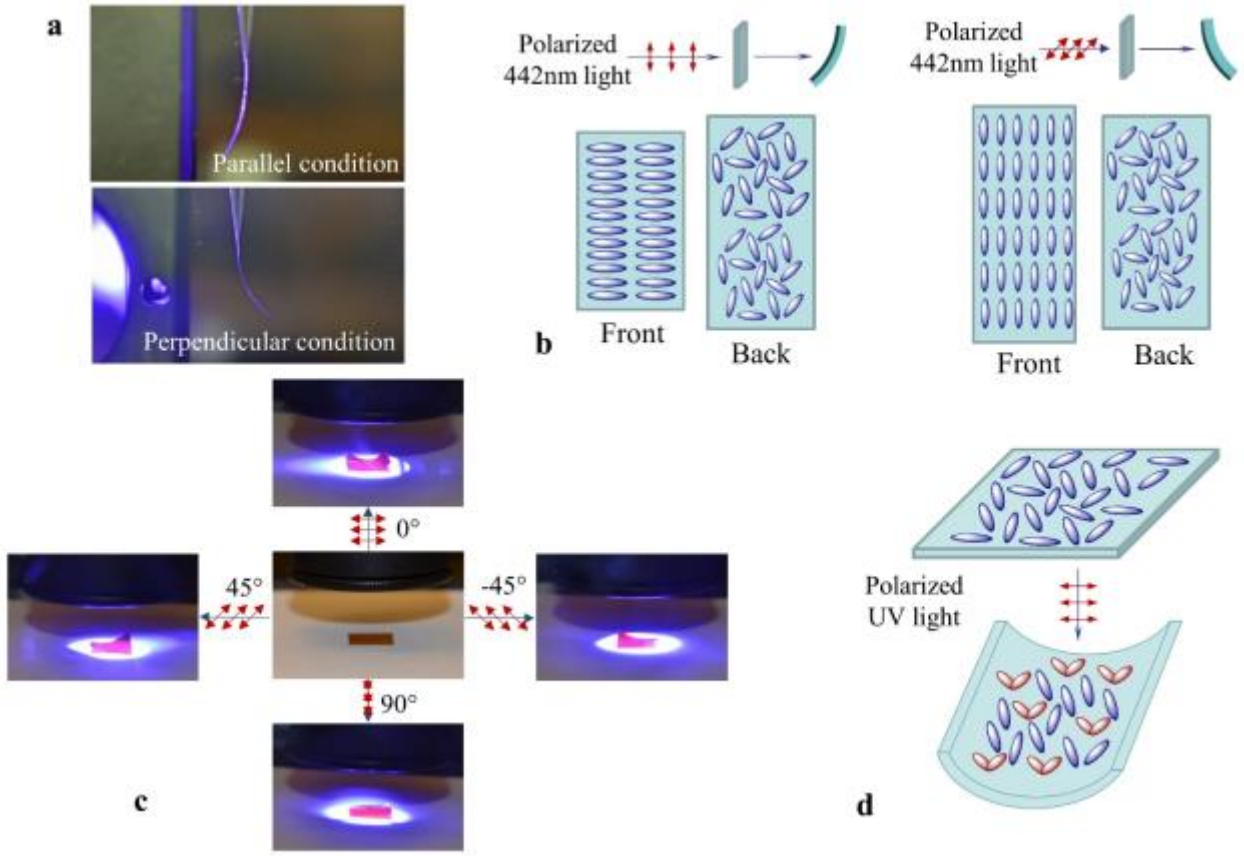

Figure 2. Photomechanical behavior of LCNs. a) Blue light induced deformation of LCN film (10 mm×1 mm×15 μm) at a light intensity of 40 mW/cm^2; top: light polarization direction parallel to the long axis of the LCN film; bottom: light polarization direction perpendicular to the long axis of the LCN film. b) Mechanism of bi-directional bending behaviors of the LCNs under blue light irradiation. c) UV light induced deformation of LCN film (10 mm×10 mm×15 μm) at a light intensity of 75.8 mW/cm^2. d) Bending mechanism of LCN film under UV irradiation.

3.3 Shape Memory Behavior

LCNs are able to exhibit large dimensional changes because of the macroscopic orientation of the LC domains. Figure 3a shows the static tensile behavior of the investigated LCNs. The force-strain curve exhibited a plateau region, indicating a polydomain-monodomain (P-M) transition of the LC phase, where all the LC domains were rotating and oriented in response to the applied mechanical force.The orientation of the LC domains was confirmed by *ex-situ* 2D SAXS/WAXS experiments shown in Figure 3d and electron scattering patterns collected using transmission electron microscopy (TEM) shown in Figure 3e. For upstretched LCN film, two concentric rings were observed from the scattering pattern, indicating the presence of a smectic LC phase. The inner, sharp ring (q = 3.8 nm^{-1}, d = 16.3 Å) was a result of the scattering from the periodic layers of the smectic structure. The outer, diffuse scattering ring (q = 14.3 nm^{-1}, d = 4.4 Å) was attributed to the scattering of neighboring mesogens in the smectic layers. Upon mechanical stretching, the inner and outer rings split into two pairs of scattering arcs with non-uniform intensity distribution in the meridional and equatorial direction,

respectively, indicating that the LC domains were aligned along the direction of the mechanical stretching. The LCNs' degree of orientation increased significantly during the P-M transition, as indicated by the change in azimuthal intensity distribution of the 2D SAXS/WAXS patterns (Supplementary Figure S8). The morphology of the oriented LC domains was further investigated using electron energy loss spectroscopy (EELS) and energy filtered TEM (EFTEM). Figure 3f shows the EFTEM images of as-prepared LCN films at strain levels of 0 % (top) and 400 % (bottom) collected using zero-loss peak in EELS spectrum (Supplementary Figure S9). The contrast between LC and amorphous domains increased significantly after mechanical stretching. Similar behavior was also observed using dark field TEM imaging technique shown in Figure 3g. Using the reversible order-disorder transition, the reversible shape change of the LCNs was characterized by cyclic thermomechanical tensile tests, shown in Figure 3b.. In the experiment, the LCN film was heated to 140 °C (above T_{lc}), and then a constant force of 0.01 N was applied. Then the temperature was decreased to 80 °C at a cooling rate of 1 °C/min and then increased to 140 °C again at a heating rate of 1 °C/min. The strain of the LCN film was measured during the temperature cycling. The strain of the LCN increased during the cooling process, which was attributed to the formation and orientation of the LC domains. During the heating process, however, the strain deceased, indicating a contraction of the LCN film caused by the smectic-isotropic phase transition of the LC domains. Because of the reversible nature of the LC phase transition, this reversible shape change can be repeated several times. Cyclic thermomechanical tensile tests were also performed at different force levels to investigate the LCN's sensitivity to applied force. Three stress levels were examined and the results are shown in Figure 3c. Generally, the maximum strain of the LCN increased with the increasing mechanical force, which was attributed to a higher degree of orientation of the LC domain. However, when tested under an axial force of 0.04 N, the shape change of the LCN cannot be fully recovered, indicating slippage of polymer chains in the network.

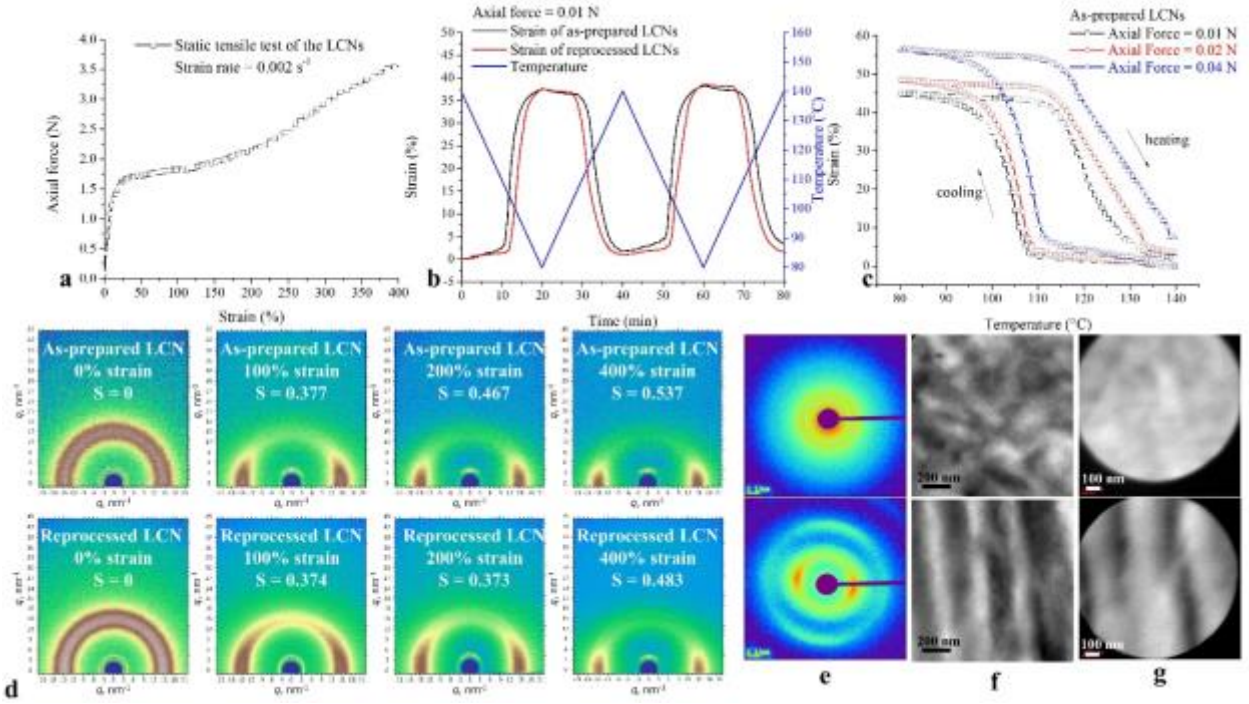

Figure 3. Thermomechanical properties of LCNs. a) Static tensile behavior of LCN film exhibiting polydomain-monodomain transition. b) Cyclic thermomechanical tensile tests of as-prepared and reprocessed LCN film. c) Cyclic thermomechanical tensile tests of as-prepared LCNs at different force levels. d) Two-dimensional X-ray scattering patterns of as-prepared and reprocessed LCN films at different strain levels (from left to right 0 %, 100 %, 200 %, and 400 %). e) Electron scattering patterns of as-prepared LCN films at strain levels of 0 % (top) and 400 % (bottom). f) Energy filtered transmission electron microscopy images of as-prepared LCN films at strain levels of 0 % (top) and 400 % (bottom) collected using zero-loss peak in electron energy loss spectroscopy spectrum. g) Dark filed TEM imaging of as-prepared LCN films at strain levels of 0 % (top) and 400 % (bottom).

Taking advantage of the reversible nature of the LC phase transition, the LC domains can be used as switching segments for shape memory applications. Figure 4a illustrates a thermally induced LC phase transition that was expressed as a change in transparency of the LCN film when the material was heated above T_{lc} (Supplementary Video S5). The two reversible transitions of the LCNs (T_g and T_{lc}) allowed for the design of a material with triple shape memory behavior, see figure 4b. For triple shape memory polymers, the permanent shape of the material is determined by the chemical crosslinks of the network, whereas two temporary shapes can be remembered through different switching domains which act as physical crosslinks to fix the deformed shapes.[31] To demonstrate the triple shape memory behavior of the LCN, an LCN box was heated to 140 °C to remove the LC phase. Then the material was flattened upon cooling to 85 °C to adopt a first temporary shape. This shape could be retained at 85 °C because of the restriction of the LC domains formed upon cooling. The material was then folded at 85 °C to adopt a second temporary shape and cooled to room temperature. The first shape recovery process (unfolding) was achieved when the material was heated back to 85 °C and became an LC rubber, shown in Figure 4c and Supplementary Video S6. Following the first shape recovery, the second shape recovery process (re-assembling) was achieved at 140 °C, when the material became an amorphous rubber when the restriction of the LC phase was removed, shown in Figure 4d and Supplementary Video S7. A quantified triple shape memory experiment is demonstrated in Figure 4e. It is noteworthy that compared to the glass transition, the LC phase transition is more suitable for shape memory applications due to the large dimension change caused by the LC orientation and their sensitivity to small forces.

The LC phase transition can also be induced by UV irradiation as shown in Figure 4f. However, here the LC phase transition was mainly caused by a photo-thermal effect rather than a photochemical effect (trans-cis isomerization) observed in the case of bending behaviors. In other words, the UV light was strongly absorbed by the azobenzene molecules and converted to thermal energy thus inducing LC phase transition (Supplementary Video S8). Supplementary Video S9 and S10 demonstrate UV-induced triple shape memory behavior of the LCNs. Figure 4g and 4h illustrate the consecutive shape recovery processes (unfolding and re-assembling) of the LCNs. Compared to thermally induced shape memory, the use of light offers multiple levels of control, i.e., via wavelength, intensity, position, and polarization. The strong photo-thermal response of the material can also be used for other applications such as self-healing and stress relaxation.

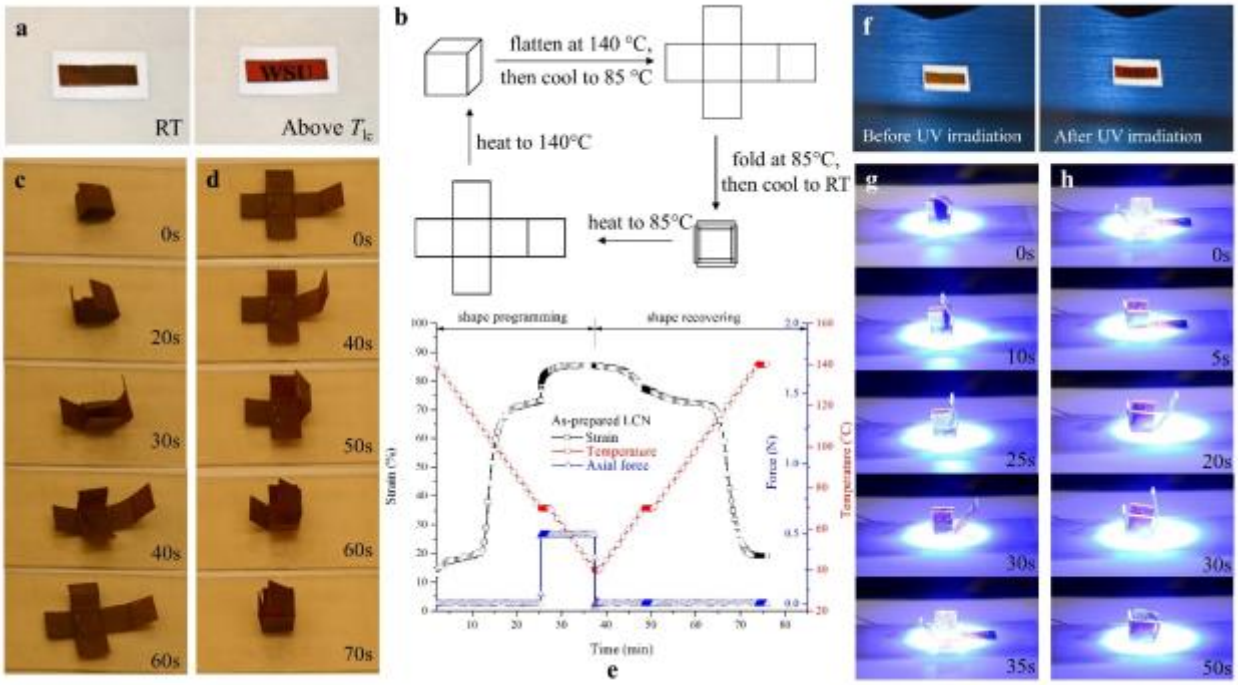

Figure 4. Triple shape memory properties of LCNs. a) Demonstration of thermally induced LC phase transition accompanied by a change in transparency. b) Demonstration of shape programming and shape recovering of LCNs. c) Thermally induced shape recovery process (unfolding) of LCNs at 85 °C caused by glass transition. d) Following the unfolding process, another thermally induced shape recovery process (re-assembling) of the LCNs at 140 °C as a result of the LC phase transition (see main text for details). e) Quantitative triple shape memory test of LCNs. f) Demonstration of UV light induced LC phase transition. g) Unfolding shape recovery process of LCNs induced by UV light. h) UV light induced re-assembling shape recovery process following previous unfolding of LCNs.

3.4 Reprocessability

Although LCNs offer remarkable properties, their practical applications are limited in part because of the difficulties in reprocessing of the materials. As a result, there has been growing interest in designing polymers using dynamic covalent chemistries. The introduction of dynamic ester bonds into epoxy or LC epoxy systems that are based on transesterification between ester and hydroxyl groups, created thermosetting materials that are re-moldable and mendable. The exchange reaction can be thermally activated at the topology freezing transition temperature (T_v)[27]. At temperatures below T_v, the exchange reaction is extremely slow so that the material exhibits a fixed topology and behaves like a permanently crosslinked thermoset, while at temperatures above T_v, the ester bonds undergo fast breaking and reforming, thereby allowing for the rearrangement of the thermoset's topology. Following this approach, we introduced this unique functionality to the LCNs under investigation by attaching epoxy groups to the azobenzene molecules. The reaction between epoxy and acid creates ester and hydroxyl groups that are exchangeable under the influence of the transesterification catalyst TBD. The transesterification initiation temperature was determined by subjecting the LCN film to a temperature ramp under a uniaxial tensile force of 0.1 N (Supplementary Figure S10). The LCN

film started to exhibit large dimensional changes at 150 °C, indicating a fast breaking and reforming of the ester bonds. Supplementary Figure S11 shows the rate of transesterification as evaluated using cyclic thermomechanical compression tests. When the temperature was cycled between 40 and 150 °C, the LCN exhibited an increase in permanent deformation of about 1.55 µm per cycle. However, this value increased to 7.97 µm when the temperature was cycled between 40 and 200 °C, suggesting a higher rate of transesterification at higher temperatures. Figure 5a shows an application of this unique functionality. Here, the thermally induced healing of broken LCN films was achieved by hot-pressing at 200 °C for 2 hour. The healed LCN film exhibited the blue light induced bending behavior, see in Figure 5b and Supplementary Videos S11 and S12. Reprocessability of the LCNs was also investigated, where as-prepared LCN film was chopped into small pieces and hot-pressed at 200 °C for 4 h, see Figure 5c. The reprocessed LCN film exhibited thermal, liquid crystalline, and thermomechanical properties similar to those of as-prepared LCN film (Supplementary Figure S12 and S13). The reversible shape change upon temperature cycling was characterized, see Figures 3b and 5d. An initially flat LCN film was remolded to form an LCN box as shown in Figure 4. In addition, the photo-thermal properties of the LCNs allowed for the activation of dynamic ester bonds using UV irradiation, which provided a unique and more efficient way of reprocessing the material. Figure 5e shows UV-induced self-healing behavior of the LCNs. Here, scratches were significantly reduced after UV irradiation for 15 min at an intensity of 242.6 mW/cm^2.

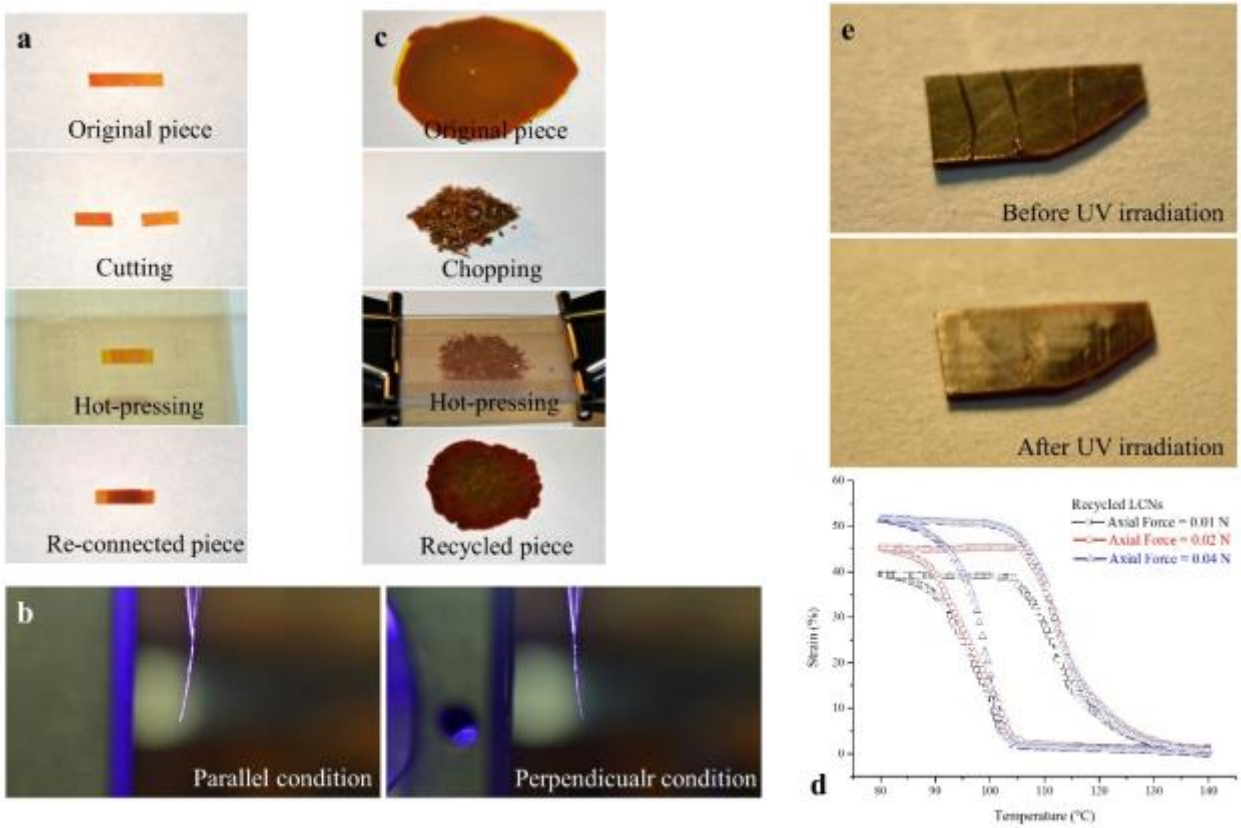

Figure 5. Reprocessability of the LCNs. a) Re-connecting broken pieces using transesterification reaction. b) Blue light induced bending of reconnected LCN film at a light intensity of 80 mW/cm^2. c) Re-processing LCN pieces by hot pressing. d) Cyclic thermomechanical tensile tests of re-processed LCN film. e) Self-healing of LCNs through exposure to UV light.

4. CONCLUSIONS

In conclusion, we developed a simple approach for the preparation of multifunctional LCNs through the combination of azobenzene chromophores, liquid crystals, and dynamic ester bonds. Our approach provides excellent compatibility of the functional building blocks and results in materials that are photo-responsive and have the ability to shift shape, undergo optical healing, and can be reprocessed. Based on this approach, LCNs can be further advanced. For example, a fourth functional building block may be incorporated into the system, e.g., magnetic-responsive[32] or infrared-responsive[33] blocks, which can be achieved by incorporating magnetic nanoparticles or single wall carbon nanotubes, respectively. In addition, functionalities can be optimized by tuning the chemistry of the material,[34] e.g., adjusting the stoichiometric ratio of AE and SA, which will change the degree of liquid crystallinity of the LCNs and result in a change in thermomechanical properties. The percentage of azobenzene chromophores can be adjusted by using an azobenzene-functionalized curing agent, which is expected to result in stronger responses of the LCNs to light stimuli.[35] Furthermore, because of their active response to external fields, the orientation of the liquid crystals can be adjusted to tailor the mechanical behavior.[36] We hope our results will contribute to the fundamental knowledge of LCNs in general and aid in the design and application of practical multifunctional systems in the future.

ASSOCIATED CONTENT

Supporting Information

Synthesis, ^{1}H NMR, and DSC scans of AE monomer (Figures S1-S3); Cure behavior and structure characterization, and thermomechanical properties of LCNs (Figures S4-S11); Characterization of reprocessed LCNs (Figures S12-S13); Blue light induced bending of LCNs (Videos S1-S4); Thermally and UV induced shape memory behavior of LCNs (Videos S5-S10); Photoresponsive behavior of reprocessed LCNs (Videos S11-S12).

AUTHOR INFORMATION

Corresponding Author

*Email: MichaelR.Kessler@wsu.edu

Notes

The authors declare no competing financial interest.

ACKNOWLEDGEMENTS

The authors would like to thank Dr. Lei Li in the School of Mechanical and Materials Engineering at Washington State University for the helpful discussion in setting up the beamline. The majority of this work was supported by the Air Force Office of Scientific Research (Award FA-9550-12-1-0108). In addition, a portion of the research was conducted at the Center for Nanophase Materials Sciences, which is sponsored at Oak Ridge National Laboratory by the Division of Scientific User Facilities, U.S. Department of Energy, managed by UT-Battelle, LLC, for the U.S. Department of Energy. Also, some of the research was sponsored by the Critical Materials Institute, an Energy Innovation Hub funded by the U.S. Department of Energy,

Office of Energy Efficiency and Renewable Energy, and Advanced Manufacturing Office, under contract DE-AC05-00OR22725 with UT-Battelle, LLC.

REFERENCES

(1) Mather, P. T.; Luo, X.; Rousseau, I. A., Shape Memory Polymer Research. *Annu. Rev. Mater. Res.* **2009**, *39*, 445-471.
(2) Behl, M.; Razzaq, M. Y.; Lendlein, A., Multifunctional Shape-Memory Polymers. *Adv. Mater.* **2010,** *22*, 3388-3410.
(3) White, S. R.; Sottos, N. R.; Geubelle, P. H.; Moore, J. S.; Kessler, M. R.; Sriram, S. R.; Brown, E. N.; Viswanathan, S., Autonomic Healing of Polymer Composites. *Nature* **2001,** *409*, 794-797.
(4) Cordier, P.; Tournilhac, F.; Soulie-Ziakovic, C.; Leibler, L., Self-healing and Thermoreversible Rubber from Supramolecular assembly. *Nature* **2008,** *451*, 977-980.
(5) Nie, Z.; Kumacheva, E., Patterning Surfaces with Functional Polymers. *Nat. Mater.* **2008,** *7*, 277-290.
(6) Wu, Z. L.; Buguin, A.; Yang, H.; Taulemesse, J.-M.; Le Moigne, N.; Bergeret, A.; Wang, X.; Keller, P., Microstructured Nematic Liquid Crystalline Elastomer Surfaces with Switchable Wetting Properties. *Adv. Funct. Mater.* **2013,** *23*, 3070-3076.
(7) Cui, J.; Drotlef, D.-M.; Larraza, I.; Fernandez-Blazquez, J. P.; Boesel, L. F.; Ohm, C.; Mezger, M.; Zentel, R.; del Campo, A., Bioinspired Actuated Adhesive Patterns of Liquid Crystalline Elastomers. *Adv. Mater.* **2012,** *24*, 4601-4604.
(8) Meitl, M. A.; Zhu, Z. T.; Kumar, V.; Lee, K. J.; Feng, X.; Huang, Y. Y.; Adesida, I.; Nuzzo, R. G.; Rogers, J. A., Transfer Printing by Kinetic Control of Adhesion to An Elastomeric Stamp. *Nat. Mater.* **2006,** *5*, 33-38.
(9) Ma, Y. J.; Dong, W. F.; Hempenius, M. A.; Mohwald, H.; Vancso, G. J., Redox-controlled Molecular Permeability of Composite-wall Microcapsules. *Nat. Mater.* **2006,** *5*, 724-729.
(10) Stuart, M. A. C.; Huck, W. T. S.; Genzer, J.; Mueller, M.; Ober, C.; Stamm, M.; Sukhorukov, G. B.; Szleifer, I.; Tsukruk, V. V.; Urban, M.; Winnik, F.; Zauscher, S.; Luzinov, I.; Minko, S., Emerging Applications of Stimuli-responsive Polymer Materials. *Nat. Mater.* **2010,** *9*, 101-113.
(11) Capadona, J. R.; Shanmuganathan, K.; Tyler, D. J.; Rowan, S. J.; Weder, C., Stimuli-responsive Polymer Nanocomposites Inspired by The Sea Cucumber Dermis. *Science* **2008,** *319*, 1370-1374.
(12) Broer, D. J.; Bastiaansen, C. M. W.; Debije, M. G.; Schenning, A. P. H. J., Functional Organic Materials Based on Polymerized Liquid-Crystal Monomers: Supramolecular Hydrogen-Bonded Systems. *angew. Chem., Int Ed.* **2012,** *51*, 7102-7109.
(13) White, T. J.; Broer, D. J., Programmable and Adaptive Mechanics with Liquid Crystal Polymer Networks and Elastomers. *Nat Mater* **2015,** *14*, 1087-1098.
(14) Ohm, C.; Brehmer, M.; Zentel, R., Liquid Crystalline Elastomers as Actuators and Sensors. *Adv. Mater.* **2010,** *22*, 3366-3387.
(15) Lendlein, A.; Jiang, H.; Junger, O.; Langer, R., Light-induced Shape-memory Polymers. *Nature* **2005,** *434*, 879-882.
(16) Ikeda, T.; Mamiya, J.-i.; Yu, Y., Photomechanics of Liquid-Crystalline Elastomers and Other Polymers. *Angew. Chem. Int. Ed.* **2007,** *46*, 506-528.

(17) Camacho-Lopez, M.; Finkelmann, H.; Palffy-Muhoray, P.; Shelley, M., Fast liquid-crystal Elastomer Swims into the Dark. *Nat Mater* **2004,** *3*, 307-310.
(18) Yu, Y. L.; Nakano, M.; Ikeda, T., Directed Bending of a Polymer Film by Light - Miniaturizing a Simple Photomechanical System Could Expand Its Range of Applications. *Nature* **2003,** *425*, 145-145.
(19) Lee, K. M.; Tabiryan, N. V.; Bunning, T. J.; White, T. J., Photomechanical Mechanism and Structure-property Considerations in the Generation of Photomechanical Work in Glassy, Azobenzene Liquid Crystal Polymer Networks. *J. Mater. Chem.* **2012,** *22*, 691-698.
(20) van Oosten, C. L.; Bastiaansen, C. W. M.; Broer, D. J., Printed Artificial Cilia from Liquid-crystal Network Actuators Modularly Driven byLight. *Nat Mater* **2009,** *8*, 677-682.
(21) White, T. J.; Serak, S. V.; Tabiryan, N. V.; Vaia, R. A.; Bunning, T. J., Polarization-controlled, Photodriven Bending in Monodomain Liquid Crystal Elastomer Cantilevers. *J. Mater. Chem.* **2009,** *19*, 1080-1085.
(22) Yamada, M.; Kondo, M.; Miyasato, R.; Naka, Y.; Mamiya, J.-i.; Kinoshita, M.; Shishido, A.; Yu, Y.; Barrett, C. J.; Ikeda, T., Photomobile Polymer Materials-Various Three-Dimensional Movements. *J. Mater. Chem.* **2009,** *19*, 60-62.
(23) Wie, J. J.; Lee, K. M.; Ware, T. H.; White, T. J., Twists and Turns in Glassy, Liquid Crystalline Polymer Networks. *Macromolecules* **2015,** *48*, 1087-1092.
(24) Lee, K. M.; Smith, M. L.; Koerner, H.; Tabiryan, N.; Vaia, R. A.; Bunning, T. J.; White, T. J., Photodriven, Flexural-Torsional Oscillation of Glassy Azobenzene Liquid Crystal Polymer Networks. *Adv. Funct. Mater.* **2011,** *21*, 2913-2918.
(25) Maeda, T.; Otsuka, H.; Takahara, A., Dynamic covalent polymers: Reorganizable polymers with Dynamic Covalent Bonds. *Prog. Polym. Sci.* **2009,** *34*, 581-604.
(26) Wojtecki, R. J.; Meador, M. A.; Rowan, S. J., Using the Dynamic Bond to Access Macroscopically Responsive Structurally Dynamic Polymers. *Nat. Mater.* **2011,** *10*, 14-27.
(27) Montarnal, D.; Capelot, M.; Tournilhac, F.; Leibler, L., Silica-Like Malleable Materials from Permanent Organic Networks. *Science* **2011,** *334*, 965-968.
(28) Pei, Z.; Yang, Y.; Chen, Q.; Terentjev, E. M.; Wei, Y.; Ji, Y., Mouldable Liquid-Crystalline Elastomer Actuators with Exchangeable Covalent Bonds. *Nat. Mater.* **2014,** *13*, 36-41.
(29) Gibbons, W. M.; Shannon, P. J.; Sun, S.-T.; Swetlin, B. J., Surface-mediated Alignment of Nematic Liquid Crystals with Polarized Laser Light. *Nature* **1991,** *351*, 49-50.
(30) Ikeda, T.; Nakano, M.; Yu, Y.; Tsutsumi, O.; Kanazawa, A., Anisotropic Bending and Unbending Behavior of Azobenzene Liquid-Crystalline Gels by Light Exposure. *Adv. Mater.* **2003,** *15*, 201-205.
(31) Behl, M.; Lendlein, A., Triple-shape Polymers. *J. Mater. Chem.* **2010,** *20*, 3335-3345.
(32) Kaiser, A.; Winkler, M.; Krause, S.; Finkelmann, H.; Schmidt, A. M., Magnetoactive Liquid Crystal Elastomer Nanocomposites. *J. Mater. Chem.* **2009,** *19*, 538-543.
(33) Kohlmeyer, R. R.; Chen, J., Wavelength-Selective, IR Light-Driven Hinges Based on Liquid Crystalline Elastomer Composites. *Angew. Chem. Int. Ed.* **2013,** *52*, 9234-9237.
(34) Li, Y.; Pruitt, C.; Rios, O.; Wei, L.; Rock, M.; Keum, J. K.; McDonald, A. G.; Kessler, M. R., Controlled Shape Memory Behavior of a Smectic Main-Chain Liquid Crystalline Elastomer. *Macromolecules* **2015,** *48*, 2864-2874.
(35) Kondo, M.; Sugimoto, M.; Yamada, M.; Naka, Y.; Mamiya, J.-i.; Kinoshita, M.; Shishido, A.; Yu, Y.; Ikeda, T., Effect of Concentration of Photoactive Chromophores on Photomechanical Properties of Crosslinked Azobenzene Liquid-crystalline Polymers. *J. Mater. Chem.* **2010,** *20*, 117-122.

(36) Ware, T. H.; McConney, M. E.; Wie, J. J.; Tondiglia, V. P.; White, T. J., Voxelated Liquid Crystal Elastomers. *Science* **2015,** *347*, 982-984.

TABLE OF CONTENTS GRAPHIC